3-2016

Fire disturbance effects on land surface albedo in Alaskan tundra

Nancy H. F. French
Michigan Technological University

Matthew A. Whitley
Michigan Technological University

Liza K. Jenkins
Michigan Technological University

AGU PUBLICATIONS

JGR

Journal of Geophysical Research: Biogeosciences

RESEARCH ARTICLE
10.1002/2015JG003177

Key Points:
- A significant decrease in MODIS-derived albedo was found as a result of tundra fire
- Albedo was impacted more at the severe site than at the moderately burned site
- Tundra fire caused a substantial increase in surface shortwave forcing

Supporting Information:
- Supporting Information S1

Correspondence to:
N. H. F. French,
nhfrench@mtu.edu

Citation:
French, N. H. F., M. A. Whitley, and L. K. Jenkins (2016), Fire disturbance effects on land surface albedo in Alaskan tundra, *J. Geophys. Res. Biogeosci.*, *121*, 841–854, doi:10.1002/2015JG003177.

Received 7 AUG 2015
Accepted 19 FEB 2016
Accepted article online 22 FEB 2016
Published online 16 MAR 2016

Fire disturbance effects on land surface albedo in Alaskan tundra

Nancy H. F. French[1], Matthew A. Whitley[1,2], and Liza K. Jenkins[1]

[1]Michigan Tech Research Institute, Michigan Technological University, Ann Arbor, Michigan, USA, [2]Department of Geology and Geophysics, University of Alaska Fairbanks, Fairbanks, Alaska, USA

Abstract The study uses satellite Moderate Resolution Imaging Spectroradiometer albedo products (MCD43A3) to assess changes in albedo at two sites in the treeless tundra region of Alaska, both within the foothills region of the Brooks Range, the 2007 Anaktuvuk River Fire (ARF) and 2012 Kucher Creek Fire (KCF). Results are compared to each other and other studies to assess the magnitude of albedo change and the longevity of impact of fire on land surface albedo. In both sites there was a marked decrease of albedo in the year following the fire. In the ARF, albedo slowly increased until 4 years after the fire, when it returned to albedo values prior to the fire. For the year immediately after the fire, a threefold difference in the shortwave albedo decrease was found between the two sites. ARF showed a 45.3% decrease, while the KCF showed a 14.1% decrease in shortwave albedo, and albedo is more variable in the KCF site than ARF site 1 year after the fire. These differences are possibly the result of differences in burn severity of the two fires, wherein the ARF burned more completely with more contiguous patches of complete burn than KCF. The impact of fire on average growing season (April–September) surface shortwave forcing in the year following fire is estimated to be 13.24 $\pm 6.52\ \mathrm{W\,m^{-2}}$ at the ARF site, a forcing comparable to studies in other treeless ecosystems. Comparison to boreal studies and the implications to energy flux are discussed in the context of future increases in fire occurrence and severity in a warming climate.

1. Introduction

Fire in arctic tundra ecosystems is generally considered uncommon; the incidence of fire across the Alaskan Arctic region is considerably less than in the adjacent boreal forest region [*Racine et al.*, 1985; *Rocha et al.*, 2012; *French et al.*, 2015]. Fire's influence on ecosystems has been explored and documented for only a few cases and in limited locations [e.g., *Racine et al.*, 1987, 2004, 2006; *Jandt et al.*, 2008; *Bret-Harte et al.*, 2013], although attention to arctic ecosystems is increasing as the region rapidly changes due to climate warming and increased human presence [*Arctic Climate Impact Assessment*, 2004; *Huntington et al.*, 2007]. Fire and other disturbance can dramatically modify ecosystem structure and function impacting energy exchange in the near term and creating conditions which can persist to effect energy balance and ecosystem functioning over multiple years [*Chambers et al.*, 2005; *Rocha and Shaver*, 2011a; *Jin et al.*, 2012]. Landscape-scale disturbances of large magnitude, or if occurring across large spatial extents, have the ability to influence regional and possibly global systems, especially if the effects are persistent [e.g., *Racine et al.*, 1987, 2004, 2006; *Sturm et al.*, 2005; *Jandt et al.*, 2008; *Bret-Harte et al.*, 2013]. Therefore, the role of fire in arctic energy exchange is potentially important as the region experiences a rapid transition brought on by climatic warming and human use.

Studies of fire and albedo in the boreal have provided insight into the important role fire has on ecosystem modifications that influence energy exchange [*Betts and Ball*, 1997; *Chambers et al.*, 2005; *Randerson et al.*, 2006; *Jin et al.*, 2012; *Huang et al.*, 2015]. In an earlier study of boreal ecosystems by *French* [2002], immediate postfire summertime albedo was reduced slightly due to the presence of char, but long-term (5–10 years postfire) albedo increased in forested ecosystems and showed small increase or no change from the preburn in shrub-dominated sites. In boreal forest landscapes, fire initiates a transition from late successional forests dominated by conifers to a younger early successional forests of aspen, birch, and deciduous shrub cover types [*Chapin et al.*, 2006]. These younger sites have a substantially different energy exchange profile than the spruce-dominated older sites. With the loss of tree canopies, boreal fire dramatically modifies the vegetation surface, including an overall increase in summertime albedo and a decrease in surface roughness, which have a strong influence on energy exchange. Transition to shrub cover and low-stature trees during boreal forest fire creates areas of exposed snow pack resulting in winter and early springtime albedos that are much higher than the preburn intact forest thereby influencing energy exchange year round [*Eugster et al.*, 2000].

The impact of fire on albedo in tundra burned sites differs in fundamental ways from what has been observed in boreal regions [*Eugster et al*., 2000; *French*, 2002; *Chambers et al*., 2005]. Surface structure in shrub-dominated boreal sites and in tundra settings impacted by fire is not as dramatically altered from the disturbance. In boreal forest settings, surface structural changes dominate the modification of surface energy balance from fire, while in treeless landscapes change in albedo is the main driver of fire-induced energy balance alterations [*Chambers et al*., 2005; *Rocha and Shaver*, 2011a]. Because fire does not often create a dramatic long-term change in vegetation structure, apparent recovery to preburn conditions, including albedo recovery, happens within 4 years or often less [*Loboda et al*., 2013; *Jenkins et al*., 2014]. While the boreal forest energy profile is impacted by fire for decades [*Betts and Ball*, 1997; *French*, 2002; *Jin et al*., 2012; *Huang et al*., 2015], energy balance in treeless tundra sites is most influenced by fire through its short-term impact on growing season shortwave energy exchange, which can directly modify ground, surface, and air temperatures, although there is only a small number of studies to support this [*Chambers et al*., 2005; *Rocha and Shaver,* 2011a].

Albedo is defined as the ratio of reflected solar radiation to incoming solar radiation. It can be estimated as the integrated amount of shortwave solar reflectance measured across the 0.3 to 5.0 μm spectral range using remote sensing systems that measure reflected solar radiance energy, such as handheld or tower-mounted in situ instruments, airborne-deployed sensors, or electrooptical sensing systems onboard satellite platforms. Albedo controls surface shortwave net radiation flux as a function of incoming solar radiation [*Jin and Roy*, 2005; *Monson and Baldocchi*, 2014]. Land surface albedo provides a measure of the amount of solar radiation reflected and absorbed by the land and therefore is an important parameter for assessing the energy balance of a site. Land surface albedo during the summer is particularly important in high northern latitudes because of the unique energy balance conditions of the high latitudes due to low solar angles, long summer days and short winter days, and the presence and dynamics of perennially frozen ground (permafrost) which influences ground thermal conditions and therefore site ecology and energy exchange. Indeed, the amount of shortwave energy absorbed at the surface, rather than reflected due to the albedo, can contribute to changes in permafrost status and provides an important trigger to permafrost degradation and deepening of the active layer [*Rocha et al*., 2012].

Surface shortwave forcing (SSF) is the change in shortwave radiative flux at the surface due to changes in albedo and describes the fate of the solar energy that can modify ground, surface, and air temperatures. *Jin et al*. [2012] found SSF to be considerably reduced in many fire-disturbed boreal forest ecosystems driven primarily by higher albedo vegetation replacing the prefire forests. The study followed similar results showing that change in boreal forest cover type from fire causes a net increase in albedo and reduction in shortwave radiative forcing over long time periods [*Betts*, 2000; *French*, 2002; *Randerson et al*., 2006]. Results from tundra, however, show an increase in SSF [*Rocha et al*., 2012] and that fire in temperate grassland ecosystem reduces the high albedo of unburned herbaceous cover in the first year following the fire leading to a dramatic positive change in SSF [*Jin and Roy*, 2005].

Changes to the energy cycle from modification of albedo by fire are amplified in boreal and arctic settings due to the presence of permafrost and role of SSF in ground warming and permafrost degradation [*Jones et al*., 2009; *Grosse et al*., 2011; *Rocha and Shaver*, 2011a; *Rocha et al*., 2012]. Growing season ground and surface energy balance play an important role in the biological functioning of an ecosystem leading to impacts on vegetation structure and the cycling of water, nutrients, carbon, and other trace gases at local and regional scales [*Swann et al*., 2010]. SSF is generally higher in the arctic summer than in other regions, but spatial and temporal variability is not well documented, and these values are needed for modeling global energy exchange and ecosystem dynamics. Monitoring albedo at fire-disturbed sites can provide a direct measurement of a key energy balance metric of consequence to site and regional-wide energy balance, and these measurements can provide vital information for quantifying metrics used in ecosystem modeling and in global climate models. Previous research on the role of fire in energy balance in tundra sites has provided some information on the general impact [*Rocha and Shaver*, 2011a*; Rocha et al*., 2012], but the role of fire severity in albedo modification has not had specific attention. An assessment of the impact of fire variability due to the severity of fire on local-scale albedo is essential to understand the short- and long-term effects to ecosystems and climate.

This study provides an assessment of space-based albedo monitoring in treeless sites at very high northern latitudes (above 68°N) that have been disturbed by fire. Using albedo products from the Moderate Resolution

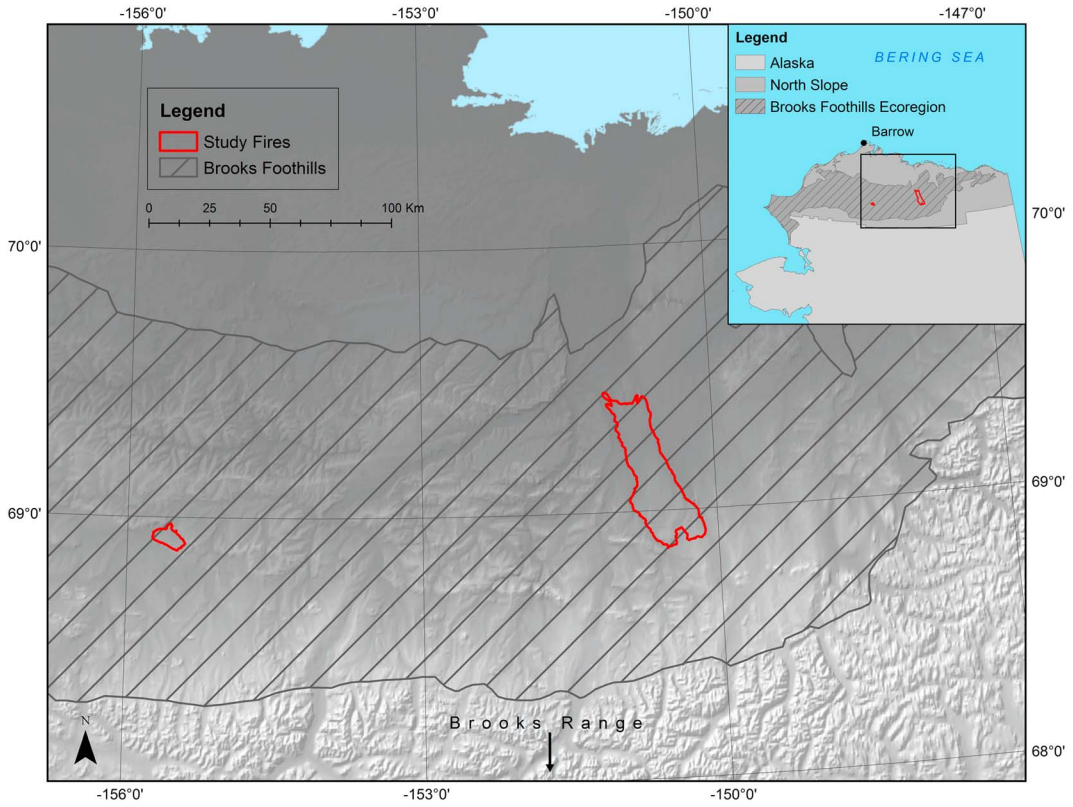

Figure 1. The study area encompasses the ARF and KCF, which both lie within the Brooks Foothills Ecoregion as delineated in the Unified Ecoregions of Alaska [*Nowacki et al.*, 2001].

Imaging Spectroradiometer (MODIS; http://modis.gsfc.nasa.gov/data/dataprod/mod43.php), changes in albedo at two fire-disturbed tundra sites in Alaska were compared to assess the magnitude of albedo change and the longevity of impact of fire on land surface albedo. Two sites were analyzed in order to compare differences due to fire severity and duration and review the possible differences in the impact fire can have on albedo in the arctic tundra region of Alaska. Extrapolation of the results to consider the impact of albedo changes from fire on shortwave forcing is discussed to postulate how increases in the extent and severity of fire may impact SSF and therefore energy balance in these ecosystems.

2. Methods

2.1. Study Area

The 2007 Anaktuvuk River Fire (ARF) and the 2012 Kucher Creek Fire (KCF) are the focus of this study. These are two of the largest recent fires on the North Slope of Alaska and represent a large, severe tundra fire and a smaller, moderately burned fire, respectively (Figure 1). They both occurred on relatively flat and mainly upland tundra sites in the Foothills Ecoregion of the Brooks Range according to the Unified Ecoregions of Alaska [*Nowacki et al.*, 2001]. Fire perimeters were obtained from the Alaska Interagency Coordination Center Large Fire Database [*Kasischke et al.*, 2002]. The sizes of these fires (ARF: 1039 km^2 and KCF: 76 km^2) are conducive to analysis with the MODIS 500 m pixel size. Both fires are contained within the swath boundary of MODIS tile h12v02 and away from the swath edge. The 2007 Kuparak Fire is also within the h12v02 MODIS tile, but its size (7 km^2) and geometry yielded no pixels completely within the fire boundary and were thus excluded from analysis.

The land cover within both fire perimeters consists of moist acidic tundra dominated by *Eriophorum vaginatum* tussocks and dwarf shrubs $<$40 cm tall. Mosses are also abundant, and grasses, forbs, and lichens can be found. Plant cover is nearly continuous, with 80–100% cover [*Circumpolar Arctic Vegetation Map Team*, 2003]. The underlying soil is acidic and cold due to ice-rich permafrost and a shallow active layer. The landscape is fairly contiguous, wherein most of the foothills ecoregion has the same tussock tundra landscape. Based

Figure 2. Photographs from (left) the 2007 Anaktuvuk River Fire (ARF) taken July of 2008 and (right) the 2012 Kucher Creek Fire taken August of 2012. The ARF site shows severe burning with few patches of unburned, while the KFC photo shows patches of moss and unburned vegetation indicating a moderate burn severity.

on published information regarding ARF [*Jones et al*., 2009] and in situ assessments at KCF (L. K. Jenkins, unpublished data on depth of burn and severity, 2012), the KCF was a more moderate burn than ARF. ARF is documented as a severe fire, while evidence from site visits by the authors and viewing of postfire Landsat images confirms a patchier and less severe fire at KCF. Both fires had patches of unburned tundra, as characteristic of fires in this region, but ARF experienced fewer unburned patches, greater depth of burn, and more complete consumption of tussocks and shrubs than KCF (Figure 2). To understand the impact of the fire to vegetation, an assessment of peak summer MODIS Enhanced Vegetation Index (EVI) was made using the MODIS subsetting tool found at the Oak Ridge National Lab Distributed Active Archive Center (ORNL-DAAC; https://daac.ornl.gov/MODIS/).

2.2. Ancillary and Remote Sensing Data

The MODIS albedo data set used in the analysis, MCD43A3, provides a 500 m composite of both directional hemispherical reflectance (black-sky albedo) and bihemispherical reflectance (white-sky albedo). Both Aqua and Terra satellite data are incorporated into the data set, making MCD43A3 a combined MODIS product. The composites are produced every 8 days but contain 16 days of data acquisition [*Strahler et al*., 1999]. The algorithm used to make the composites uses data before and after any given date. However, days closer to the given date are emphasized, in order to make the composite more representative of the middle day. The Collection 005 MODIS bidirectional reflectance distribution function (BRDF) and Albedo products have attained a stage 3 validation [*Strahler et al*., 1999].

The MODIS albedo product MCD43A3 consists of reflectance measurements in seven MODIS spectral bands, as well as visible (VIS) 0.3–0.7 μm, near-infrared (NIR) 0.7–5.0 μm, and shortwave (SW) 0.3–5.0 μm broadband albedo estimates, the latter covering the full solar reflectance region [*Strahler et al*., 1999]. Though the MODIS albedo product includes reflectance for seven MODIS bands, only the broadband albedo products were included in this analysis. To capture a substantial preburn sample, data from 2003 to 2013 were analyzed.

A full model inversion to obtain albedo reflectance that results in the top quality processing can be attempted "if at least seven cloud-free observations of the surface are available during a sixteen-day period" [*Schaaf et al*., 2002]. Persistent cloud cover limits the availability of data, as it is a problem associated with all electrooptical remote sensors [*Stow et al*., 2004]. However, because of the high latitude of the region, the near-polar orbit of the Terra and Aqua satellites can make up to four observations a day [*Schaaf et al*., 2002], which means an albedo measurement could theoretically be made with only 2 days of data if each day returned four cloud-free scenes. Furthermore, lower quality processing (magnitude inversion processing) can be made with as little as three observations, suggesting that a 16 day composite could potentially be made from 1 day of observations. In the magnitude inversion processing, a priori baselines of recent BRDFs are used in the algorithm to account for the dearth of observations. It may be possible that the magnitude inversion processing rejects burned pixels if the a priori baselines do not include a fire. For these reasons, only the highest quality full inversion pixels were selected for analysis, despite the fact that there is evidence to suggest that lower quality data are accurate [*Wang et al*., 2012].

The quality control bands associated with the MODIS albedo product are available separately under the moniker MCD43A2. Identical in extent and temporal resolution, the MCD43A2 quality product provides

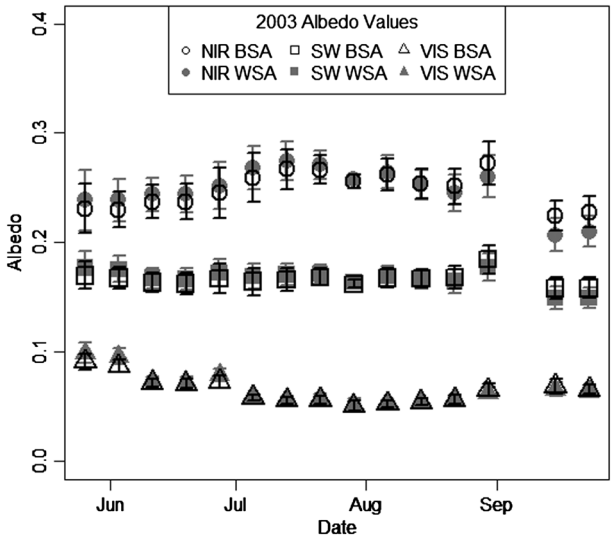

Figure 3. Boxplots of mean and standard deviation of white-sky albedo (WSA) and black-sky albedo (BSA) from late May to mid-September of 2003 of snow-free, unburned tundra (2003 had no data of sufficient quality prior to late May). The plots show the overlap between the WSA and BSA in the near-infrared (NIR), shortwave (SW), and visible (VIS) spectral ranges. When the sample spread is taken into consideration, WSA and BSA measurements are indistinguishable, and thus, the average of the two estimates was used in this study as an approximation of actual albedo.

detailed metadata and quality information. The quality product includes four science data sets (SDS) that describe general albedo quality, snow cover, ancillary data, and MODIS band quality. These bands are paramount in ensuring high-quality albedo measurements and thus were used to pare the data down to only the highest quality, snow-free, water-masked samples. Specifically, the albedo quality, snow cover, land cover, and solar zenith angle at local solar noon quality flags were used.

2.3. Albedo Data Processing and Analysis

High northern latitudes pose a challenge to collect reliable albedo data because of the high solar zenith angles encountered during the winter months. Many, including the Land Processes Distributed Active Archive Center, warn of error in albedo data with solar zenith angles above 70° [*Strahler et al.*, 1999; *Stroeve et al.*, 2005; *Wang et al.*, 2012]. Though data with solar zenith angles above 70° are not completely unreliable—*Wang et al.* [2012] note solar zenith angles up to 80° that perform well in Barrow, AK (71.2956°N, 156.7664°W)—the consensus is that the best quality data have solar zenith angles below 70°. To ensure high-quality data, the solar zenith angle at local solar noon quality flag within the ancillary SDS was used to determine the dates during which the solar zenith angle is below 70° at these sites, which lie between 68.5°N and 69.5°N latitude (see Figure 1). Based on these criteria, data before 21 March (Julian day (JD) 81) and after 21 September (JD 265) have unreliable solar zenith angles and therefore were excluded from analysis. This left a maximum of 24 MODIS 8 day composites available for analysis in each year, though further quality processing to exclude snow, water-dominated, and other low-quality pixels lowered this number to between 8 and 16 scenes each year with usable pixels and the first day of qualifying data JD 137 (16 May; Table S1 in the supporting information). Processing the data to the highest possible quality left 62,194 pixels in the ARF and 4012 pixels in the KCF over the span of 11 years. This is an average of 10% of the ARF and 11% of the KCF area per scene that was available for analysis. Analysis was performed with all qualifying 8 day composite pixels that were fully within the fire boundaries during the 11 year MODIS data record; pixels were pooled to an average value for each year for all analyses due to the limited number of pixels available monthly (see Table S1). Due to the stability of albedo across the study period (JD 137–265), pooling the data for each year provides a valid estimate of growing season albedo change from fire for this study (Figure 3).

The MODIS albedo product provides both black-sky albedo and white-sky albedo, while the actual bidirectional reflectance albedo (i.e., "blue-sky" albedo) lies somewhere in between the two [*Stroeve et al.*, 2005; *Liu et al.*, 2009]. The blue-sky albedo can be thought of as a ratio of black-sky radiation to white-sky radiation in the atmosphere and can be calculated using aerosol optical depth at the time of the albedo measurement to determine the ratio. However, the black-sky and white-sky albedo measurements in this analysis overlap within the spread of the sample so they do not exhibit distinct values (Figure 3). To simplify the process, a 1:1 ratio of black-sky radiation to white-sky radiation in the atmosphere was assumed, and the two albedo returns were averaged to produce a single value representing blue-sky albedo and were reported here as "albedo."

The 2007 ARF burned from 16 July to 9 October (85 days), and the 2012 KCF burned from 18 June to 2 July (14 days) [*Alaska Interagency Coordination Center*, 2015]. These durations are important to consider alongside the temporal resolution of the MODIS 8 day composite product used in this study. ARF burned well past the

Table 1. Number of Scenes and Pixels Sampled the Year of Each Fire Within the Anaktuvuk River Fire (ARF) and Kucher Creek Fire (KCF) Before, During, and After the Fire Events[a]

				Available			
Fire	Year of Fire	Fire Size (km^2)	Number of	Before Fire	During Fire	After Fire	Total
ARF	2007	1039	Scenes	7	9	0	16
			Pixels	3553	5098	0	8651
KCF	2012	76	Scenes	3	2	4	9
			Pixels	59	43	79	181

[a]The ARF burned from 16 July (Julian day 197) to 9 October (Julian day 282), and the KCF burned from 18 June (Julian day 169) to 2 July (Julian day 183).

time that reliable albedo retrievals were possible in mid-September; thus, the earliest scenes in 2008 are the first images showing the entire fire extent, as the latest in 2007 was prior to extinguishment. In contrast, the KCF was an early season fire and was extinguished on 2 July, leaving a substantial number of scenes after the fire in 2012. Table 1 presents the number of scenes and pixels available before, during, and after the fires at Anaktuvuk River and Kucher Creek in their respective years.

The MODIS data were reprojected to an Albers Conic Equal Area projection for analysis. The compressed quality flags were unpacked and bit shifted using the Land Data Operational Product Evaluation Tools [*Roy et al*., 2002]. Data were limited to those with only the highest quality full BRDF inversions, and subpar and magnitude inversion data were masked out. The data were further masked with the land cover flags to remove all water features and leave only pixels classified as land. However, because of the MODIS spatial resolution, subpixel mixing inevitably included small lakes and streams on the tundra. Data were also masked to exclude snow return albedos, as snow cover on the tundra is variable and has a very high albedo. Finally, data above the maximum theoretical value of 1 and below the theoretical minimum of 0 were removed.

A sample of unburned pixels outside of the fire boundaries was obtained to use as a control. These pixels were selected at random from the adjacent tundra outside the fire boundaries within the Brooks Foothills ecoregion. To be considered in this context, a pixel must have met the following biophysical requirements: the area within the pixel must not have burned in recent history or overlap in any part with previous fires on record; the pixels selected required a similar slope and elevation to those within each fire region, respectively; and pixels needed to encompass only the same type of tundra (defined by the CAVM classification G4) [*CAVM Team*, 2003]. Pixels located within river channels in the region were also excluded. The number of random, unburned pixels collected for each fire was commensurate with the yearly number of pixels within each fire region over the 11 year period; Table S1 shows the albedo sample set's number of pixels and scenes used. All of these pixels fell within 100 km of their respective fires.

An analysis of variance (ANOVA) was conducted on the albedo returns to assess recovery after fire. A two-way additive effects ANOVA was implemented for each spectrum of each fire that predicts albedo as a function of the year in which the burn occurred (the year effect) and if burned or unburned (the burn effect). The difference between the unburned tundra albedos inside and outside the fire perimeter before the fire year was also taken into account to control for inherent differences between the tundra regions sampled (regional offset).

The model developed for the data is

$$X_{ik} = \mu_i + \varepsilon_{ik} \qquad k = 1,\ \ i = 1, 2, \ldots,\ \ 11 \tag{1}$$

$$X_{ik} = \mu_i + \rho + \varepsilon_{ik} \qquad k = 2,\ \ i = 1, 2, \ldots,\ i_b - 1 \tag{2}$$

$$X_{ik} = \mu_i + \rho + v_i + \varepsilon_{ik} \qquad k = 2,\ \ i = i_b, i_b + 1, \ldots, 11 \tag{3}$$

where i is the year, k is the index for unburned ($k = 1$) and burned ($k = 2$), i_b is the year in which burn occurred, μ_i is year effect, ρ is the regional offset (between burned and unburned control regions), v_i is the burn effect, and ε_{ik} is the error approximately normally distributed with variance σ^2.

Given the data model, the two-way ANOVA model is of the form

$$Y_{ik} = \mu_i + v_{ik}$$

where $k = 1$ if unburned and $k = 2$ if burned and

$$v_{ik} = 0 \qquad k = 1$$
$$v_{ik} = \rho \qquad k = 2, i < i_b$$
$$v_{ik} = \rho + v_i \qquad k = 2, i \geq i_b$$

2.4. Estimating Surface Shortwave Forcing (SSF)

Surface shortwave forcing (SSF) was estimated using the methods of *Jin and Roy* [2005] to assess the impact of albedo change from fire in the context of energy balance. SSF was calculated from the change in albedo from before the fire (α_1) to after the fire (α_2) based on the average amount of incoming solar radiation (R_{sw}) during the months with solar zenith angle above 70° (JD 81–265) in watts per unit area (W m^{-2})

$$\mathrm{SSF} = -R_{sw}(\alpha_2 - \alpha_1)$$

SSF is a measure of the impact of the burn on the shortwave energy at the surface; for this study the impact was assessed for the snow-free growing season period at 1 year following the fire for the KCF and for 1, 2, and 3 years postfire for ARF. Daily mean incoming solar radiation for this latitude from 21 March to 21 September (JD 81–265) was obtained from NASA's Modern Era Retrospective Analysis for Research and Application data [*Modern-Era Retrospective Analysis for Research and Applications*, 2013; *Huang et al*., 2015]. Daily values for the 2003 to 2013 study period were averaged to obtain growing season monthly average incoming solar radiation from April to September and assess SSF. Daily averages were considered appropriate estimates of R_{sw} for this application because MODIS is in a Sun-synchronous orbit collecting data midday local time. Because the albedo data were pooled to yearly growing season values, and interannual differences in R_{sw} are within the intra-annual variability for the study period, the average growing season R_{sw} across all study years of 183.42 ± 69.74 W m^{-2} was used to estimate the average SSF across the 6 month period of each year. The potential range in SSF was computed and is reported here based on ±1 standard deviation of the mean incoming solar radiation during the 11 year/6 month period of the study.

3. Results

The effect of the fire on albedo is shown in the boxplots of the ARF (Figure 4a), and to a certain extent in the KCF (Figure 4c), which compares the median, quartiles, and maximum/minimum albedo values across the 11 years of the analysis. In the ARF, there is a marked decrease of albedo in the years following the fire. With each successive year after the fire, the SW and NIR albedos slowly increase, until roughly 4 years after the fire, when they are comparable to the albedo values prior to the fire. However, the VIS albedo shows a decrease only in the year after the fire and by 2009 is similar to the prefire years, albeit with a higher variability in the data. When compared to the albedos of the unburned pixels (Figure 4b), the burned albedos generally have a higher variability, especially the year of the fire and several years after the fire. An exception to this occurs the year after the fire in 2008, where the albedos have a very narrow spread and little variability. In general, the NIR albedo has a wide spread, including within the sample of unburned pixels.

The KCF (Figures 4c and 4d) case provides less data after the fire than the ARF; however, similar trends are present. The decrease in albedo the year after the fire is not as extreme as that of the ARF; rather, the fire year shows the largest aberration from the previous albedos. For the fire year, the means of the SW and NIR albedos are significantly lower than the previous years, with the entire interquartile range lower than the previous years. Similar to the ARF, the year of the fire shows much variability for the three broadband albedo estimates, but contrary to the ARF, the albedos 1 year after the fire also have a fairly large spread in the data.

Annual mean burned SW albedo of the ARF is 0.086 1 year following fire (2008) and increases to 0.160 4 years later (2012). Mean SW albedo 1 year after the KCF is 0.147. The full set of albedos for all three spectral ranges is given in Table S2. Standard deviations are consistent across years and between sites. The ARF and KCF total average unburned albedos in the SW are comparable (within 1 standard deviation). When combined, the unburned samples from outside of the burn regions over the 11 year span yield average albedos of 0.165 ± 0.008 for the SW spectral range, 0.063 ± 0.005 in the VIS, and 0.250 ± 0.013 in the NIR.

The year after the fire exhibits the maximum deviation from the average unburned tundra for both the ARF and KCF (Figure 4). However, the magnitude of the change at the ARF is much larger than that of the change

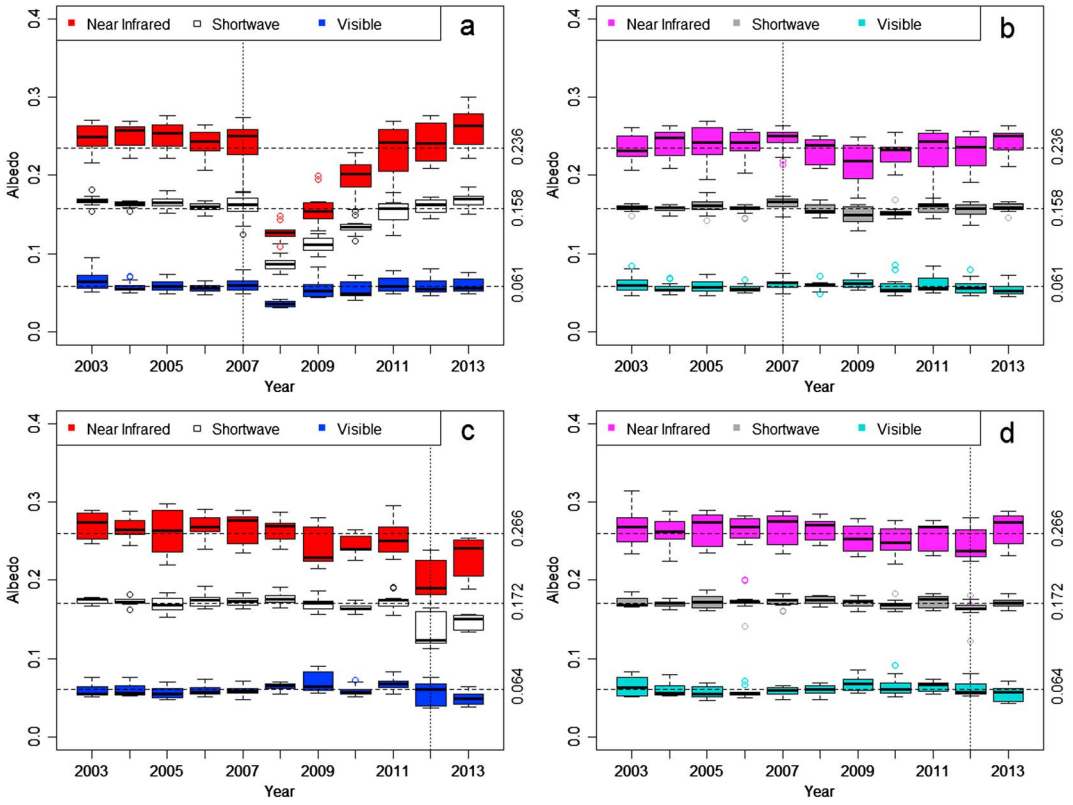

Figure 4. Boxplots showing the MODIS-derived albedo data for each year (a) within the ARF burn perimeter, (b) adjacent unburned pixels, (c) within the KCF burn perimeter, and (d) adjacent unburned pixels. Data are for of all available snow-free, high-quality pixels from 21 March to 21 September for each year; the box shows the upper and lower quartiles, and the lines show the mean (dark line) and minimum and maximum values. Fire years are marked with a vertical dashed line. The plots include horizontal dashed lines indicating the mean of unburned pixels (values shown to the right of the plots). For the year of the fires, the albedo samples from within the burn perimeters have large variability due to inclusion of both burned and unburned tundras within the annual set of samples. Due to inherent differences in the fires' chronologies mean, ARF albedo is similar to preburn, while mean KCF albedo is similar to postburn (see text).

at KCF. Table 2 presents the change in average snow-free albedo for each year postfire from the average unburned sample and resulting SSF after the fire for the ARF and the KCF. Also shown is peak MODIS-derived EVI for each year postfire. The percent albedo change calculated from the average unburned tundra adjacent to the ARF shows a 45.3% decrease in albedo in the SW, a 38.1% decrease in the VIS, and a 46.2% decrease in

Table 2. Shortwave Albedo Change at the Two Sites Computed From the Difference Between Average Burned and Unburned Tundra Albedo at 1, 2, and 3 Years After Fire; and the Average Surface Shortwave Forcing (SSF) for the 6 Month Study Period (Julian Days 81–265) Computed Based On Published Methods [*Jin and Roy*, 2005; *Huang et al.*, 2015] Assuming Growing Season Average Incoming Solar Radiation of 183.42 ± 69.74 W m^{-2}[a]

		Number of Years Postfire		
		1	2	3
ARF	Albedo Change	-0.072 ± 0.023	-0.047 ± 0.017	-0.025 ± 0.015
	SSF (W m^{-2})	13.24 ± 6.52	8.53 ± 4.46	4.56 ± 3.28
	MODIS EVI	0.14	0.23	0.34
KCF	Albedo Change	-0.025 ± 0.0094	na	na
	SSF (W m^{-2})	4.64 ± 2.47	na	na
	MODIS EVI	0.35	na	na

[a]Also shown is peak summer Enhanced Vegetation Index (EVI) computed from the 16 day MODIS composite product for pixels within each burn scar for corresponding years. Preburn EVI is 0.40 for both sites. All values include ±1 standard deviation. An annual estimate of SSF would be one half of these results assuming zero forcing in winter months. Na means not applicable.

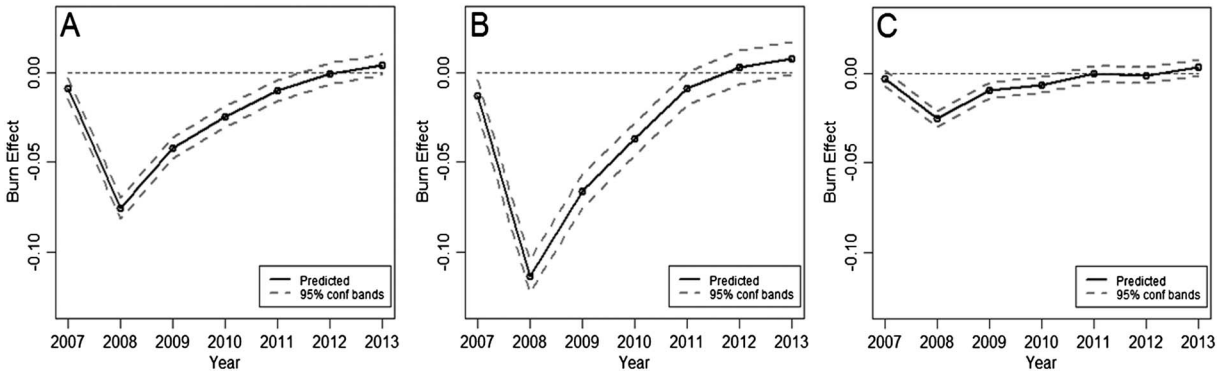

Figure 5. Model-predicted recovery after fire at ARF suggests a return to zero effect on albedo from burning after approximately 5 years in (a) the SW and 4 years in (b and c) the VIS and NIR. The 95% confidence intervals are represented by the dashed lines and the zero-effects line is represented by the horizontal dashed line. Statistical analyses found that postfire albedo is predominantly a function of the fire event with limited effect due to the intrinsic variability in the spectral reflectance of unburned tundra.

the NIR. For the KCF the changes are less: 14.1% decrease in the SW, 17.3% decrease in the VIS, and 11.0% decrease in the NIR. Between the two sites, this constitutes a 31.2% difference in the SW, a 20.7% difference in the VIS, and a 35.2% difference in the NIR. Fire-induced SSF for ARF is as high as $13.24 \pm 6.52\ \mathrm{W\,m^{-2}}$ in the first year postfire and 4.56 ± 3.28 after 3 years. A similar SSF of $4.64 \pm 2.47\ \mathrm{W\,m^{-2}}$ is found after 1 year at the less severe KCF (Table 2). EVI changes predictably at both sites with a substantially lower response at the KCF than the more severe ARF.

The statistical analyses found that postfire albedo is predominantly a function of the fire event with limited effect due to the intrinsic variability in the spectral reflectance of unburned tundra. Unburned samples for both sites show slight variation over the 11 year span (Figures 4b and 4d) but nothing as drastic as the deviation caused by the fires. Differences found between the unburned samples obtained from within and outside of the burn perimeter (the regional offset) are significant only in the ARF SW and NIR albedo cases and at a minimal significance level of $p < 0.05$; in all other cases the regional offset differences are not significant. Figure 5 shows the model-predicted effect of the burn on albedo and recovery after fire for the ARF for each year following the fire. The spectral recovery after fire (return to zero effect line) is 5 years for the SW spectral range and 4 years for the NIR and VIS spectral ranges. The gradual return to preburn albedo is reinforced by the shrinking difference from average unburned albedo values shown in Table S2 and can be seen in Figure 5.

4. Discussion

4.1. Data Quality and Coverage

MODIS standard data products provide a way to assess decade-long variability and trends at broad spatial scales. In the case of albedo, MODIS provides a continuous and consistent view that has not been available through other methods, allowing assessment of the magnitude of fire's impact on site ecology and energy balance and patterns of postfire recovery. The frequent overpasses of MODIS onboard both Terra and Aqua satellites maximize the likelihood of clear scenes, and the 8 day composites provide a valuable temporal snapshot of the tundra. The spatial resolution, however, limited the scope of this study to larger fires therefore excluding small fires, which are more common in the region than the two fires used in this study [*French et al.*, 2015].

The analysis performed was limited by the availability of data, as the high latitude of the region (north of 68°N) poses several challenges for obtaining high-quality albedo data. Strict data quality management restricted the samples to approximately 10% of the potential pixels available. Chief among the challenges were the high solar zenith angles and limited solar illumination in the winter, which constrain the data used to dates between JD 81 (21 March) and JD 265 (21 September) [*Strahler et al.*, 1999; *Stroeve et al.*, 2005; *Wang et al.*, 2012]. In order to concentrate on growing season energy questions, this study focused on albedo in snow-free conditions and did not take into account the impact of disturbance on winter or early spring albedo, which has been shown to be important in other biomes [*Betts and Ball*, 1997; *Barnes and Roy*, 2010;

Jin et al., 2012]. Due to low tundra vegetation stature, the large impact of snow cover known to be of importance at fire-disturbed sites in forested regions is not as important in these treeless sites, and the impact from fire disturbance on growing season (snow-free) albedo is a more influential factor to consider [*Chambers et al.*, 2005].

For the year of the fires, albedo from within the burn perimeters shows large variability due to inclusion of both burned and unburned tundras within the annual set of samples. Incorporating a fire progression model into the analysis [e.g., *Loboda and Csiszar*, 2007; *Jones et al.*, 2009] could help identify burned versus unburned samples, but the number of high-quality burned samples in the year of the fire would likely be small because the time frame would be restricted to a small date range and smoke obscuration, thereby limiting the information gained. Because of the mixed samples, the data show a large spread about the mean within the fire year for both sites (Figure 4). The pattern of the pixels sampled in the fire year differs between the AFR and KCF sites due to inherent differences in the fires' chronologies, resulting in a different result between the two sites (mean ARF albedo is similar to preburn, while mean KCF albedo is similar to postburn). The KCF burned quickly and early in the year, while the ARF started in mid-July and burned well past the date of albedo data used in this study (22 September; Table 1). Thus, the albedo returns used in the analysis from the ARF for the year of the burn include a variety of burned and unburned samples, whereas the albedo returns obtained within the KCF for the year of the fire are primarily postfire samples. Because of these differences and the mixed samples, data from the fire year were not included in the analyses conducted in this study and the data points from the fire year shown in Figures 4 and 5 should be assessed within the context of these factors.

4.2. Albedo Trends at Tundra Burn Sites

Results show a decrease in albedo following fire and persistence for more than 3 years. This study demonstrates a more detectable change in reflectance when looking in the SW or NIR regions of the spectrum rather than just the VIS region (Figures 4 and 5). *Loboda et al.* [2013] found similar results regarding spectral response in the NIR than in VIS but found that fire-disturbed sites are not reliably detectable after the first year following fire for early season fires. The longevity of the ARF albedo aberration found in this study may be related to the severity of the burn that has been documented at this site [*Jones et al.*, 2009]. Longevity of the more moderately burned KCF could not be assessed in this study due to the limited time since burn.

The results of this study show that postfire patterns in albedo from within the ARF and the KCF were similar but differed in several ways. In both sites, albedo dropped significantly in the year following the burn; however, the drop in the ARF shortwave albedo from the average unburned baseline was 27% more than the drop in the KCF shortwave albedo from the baseline. Furthermore, for all three broadband albedo estimates the spread of data in the ARF is very narrow 1 year following the fire (as evident in Figure 4 boxplots), denoting spectral homogeneity after fire, while the spread in the KCF is much larger denoting more spectral heterogeneity. These differences most likely correspond to the severity of the two fires, wherein the ARF burned more completely with more contiguous patches of complete burn than KCF, where the consumption was more shallow and patchy (see Figure 2). There is limited satellite data after the KCF, but in subsequent years after the ARF the albedo variability increases with each successive year, suggesting a spectrally variable landscape as the tundra recovers from the fire. This study provides compelling evidence that albedo modification from fire is a function of burn severity and patchiness. Therefore, in assessing the impacts of fire on energy balance in the tundra it is important to note the overall severity of a burn, as this variable is an important driver of shortwave energy forcing.

The average MODIS-derived albedo of unburned tundra found around Anaktuvuk (0.158 ± 0.010) corresponds well to the in situ unburned albedo values reported in *Rocha and Shaver* [2011a] and the measured value of 0.155 of *Eugster et al.* [2000] for nonshrub, upland moist tussock-shrub tundra. The average unburned tundra albedo near Kucher Creek (0.171 ± 0.006) corresponds better to other classifications presented by *Eugster et al.* [2000], namely, a nonshrub, noncoastal wet meadow (i.e., sedges) classification that has an albedo of 0.175. Both of these in situ measurements were collected in Happy Valley, Alaska—a site less than 100 km to the east of the ARF. *Chambers et al.* [2005] found the average albedo of unburned tundra to be higher at 0.19 ± 0.001, but their sample site was on the Seward Peninsula, which is in a different floristic province and a more shrub-dominated tundra classification [*CAVM Team*, 2003]. Studies have shown

that MODIS generally underestimates albedo for certain plant functional types including grasslands, savannas, and cropland [*Jin et al*., 2003; *Cescatti et al*., 2012]. Because of the lack of MODIS product validation over tundra, it is possible that absolute albedo returns are underestimated in this study; however, relative albedo changes are expected to be reliable.

4.3. Implications of Albedo Changes From Tundra Fire

As reviewed above, the influence of fire on albedo in tundra burned sites differs from what has been observed in boreal regions. The albedo response in the boreal is driven mainly by a change in vegetation structure and composition that is brought on as a result of the disturbance (e.g., a shift from late successional forest to shrub and early successional species). In treeless tundra, vegetation structure is not strongly modified, so growing season albedo is driven by the introduction of char and loss of green vegetation, both of which return to preburn conditions within a few years, as confirmed by remote sensing in this study and by *Rocha et al.* [2012]. Fire-induced transition from one vegetation type to another is possible, although it has not been observed in the ARF [*Bret-Harte et al*., 2013], and would not have a strong influence on summertime reflectance, since both herbaceous tussock-dominated sites are similar to light-leaved shrub-dominated sites. Furthermore, winter and spring albedo in tundra is not expected to be dramatically changed by fire, as has been shown in studies of the boreal [*Chambers et al*., 2005; *Jin et al*., 2012]. Increasing shrub cover that has been documented for the circumpolar arctic, however, could change this situation and make winter and spring snow albedo's influence on energy exchange more complex than currently observed [*Sturm et al*., 2005; *Tape et al*., 2006; *Loranty et al*., 2011].

Despite the minimal impact on vegetation structure, albedo changes found at tundra sites following fire are of consequence to the energy flux. Differences between the two sites show that energy flux impacts are dependent on burn severity and patchiness. Immediate modification to surface energy balance in fire-disturbed sites is expected due to albedo decrease brought on with the presence of char and loss of high albedo plant material. This creates a corresponding increase in SSF, which modifies sensible heat flux, and a decrease of vegetation greenness, as detected in EVI (see Table 2 and *Rocha et al*. [2012]). In addition, disturbance subsequent to the fire includes warming of the ground which causes permafrost melt and thermokarst [*Grosse et al*., 2011]. This leads to soil moisture increase and is further exacerbated by loss of vegetation transpiration [*Jenkins et al*., 2014] further modifying the energy balance at a site. It is expected that the differences seen in both magnitude and persistence of albedo change between the severe ARF and more moderate KCF have implications for other aspects of energy balance, with a severe fire being more consequential to permafrost degradation, thermokarst, and other biophysical disturbances due (in part) to albedo change from fire.

Using the average incoming solar radiation during the 6 month period of this study and the methods of *Jin and Roy* [2005], the decrease in albedo at the severe ARF and more moderate KCF reported in this study produces an average growing season SSF of $13.24 \pm 6.52\ \mathrm{W\,m^{-2}}$ and $4.64 \pm 2.47\ \mathrm{W\,m^{-2}}$, respectively (Table 2). Assuming a zero SSF for the 6 months of winter (an assumption based on the lack of incoming solar radiation over the period), annual average SSF would be one half of what is reported in Table 2. The ARF estimate is similar to fire-caused SSF documented elsewhere, and the estimate of $4.56 \pm 3.28\ \mathrm{W\,m^{-2}}$ 3 years after the fire at ARF is higher than other studies several years postfire. *Jin and Roy* [2005] found that the albedo of unburned temperate grasslands is reduced with fire, as in this study, leading to an estimated average monthly SSF within burn sites for November (summer) of $8.93 \pm 6.84\ \mathrm{W\,m^{-2}}$ and an average annual increase of $6.23\ \mathrm{W\,m^{-2}}$ from burning. On a monthly basis, therefore, tundra fire shows more influence on summertime SSF than temperate grassland sites, and the annual averages are comparable (Table 2). Boreal studies typically show a small decrease in albedo, if any change, in the year following fire resulting in a small increase in summertime SSF and then a general decrease in SSF over subsequent years [*French*, 2002; *Jin et al*., 2012; *Huang et al*., 2015].

In general, fire in high albedo vegetation types, such as herbaceous-dominated systems, will result in a decrease in albedo. The results found at the ARF, in particular, show that severe tundra fire has the potential to substantially lower albedo and raise SSF for several years postfire during snow-free periods when energy dynamics are of great importance to ecological functioning. The results from KCF, a more moderate-severity fire that is more typical of recent tundra fires, show this general result but at a smaller magnitude (Table 2). Although this study did not include more than 1 year postfire at the KCF site, this

moderate-severity burn is expected to recover more quickly than the severe ARF, therefore causing less impact on SSF and energy flux overall.

As previously documented, apparent vegetation recovery in tundra sites, including the ARF and KCF, is relatively rapid [*Jones et al.*, 2009; *Loboda et al.*, 2013; *Jenkins et al.*, 2014]. The results from the statistical analysis from ARF agree with the assessment by *Rocha and Shaver* [2011a] that albedo and surface greenness steadily recovered to match unburned tundra by the third growing season in a moderately burned test site, while severely burned tundra was slightly lower than the unburned in the third year after fire. However, *Rocha and Shaver* [2011a] also found little to no moss recovery by the third growing season after the fire, which may take decades to fully recover [*Racine et al.*, 2004]. This is significant because moss cover immediately following fire was only 5% in severely burned tundra and 30% in moderately burned tundra at the ARF [*Rocha and Shaver*, 2011b]. This impact of fire on surface vegetation has implications to energy partitioning not revealed in the assessment of albedo, because moss insulates the soil and its loss affects ground temperature and long wave radiation [*Rocha and Shaver*, 2011a]. Likewise, lichen such as *Cladina rangiferina*—important caribou fodder—does not recover quickly following fire impacting caribou grazing for years following fire [*Jandt et al.*, 2008].

Synoptic monitoring of surface albedo with space-based remote sensing as demonstrated in this study has great value for improving our understanding of how fire in tundra regions of the far north can impact the shortwave energy balance. Models predict increased fire risk in tundra compared to past decades based on a change in climatic conditions [*Hu et al.*, 2010; *French et al.*, 2015]. This study shows that as fire increases, impacts on short-term growing season energy flux could have large and broad-scale impacts on regional energy balance due to substantial SSF increases during the growing season, leading to increased ground, surface, and near-surface air temperatures across the disturbed site. The work of *Rocha and Shaver* [2011a] provides details on other energy flux components but found less difference between severe and moderate burn sites than this study. An increase in fire area, as well as potentially more severe fires, is likely to cause larger increases in SSF across the arctic than historically with potential influence on other energy balance components as well. Sites with frequent repeat burning would experience high SSF over longer periods with more dramatic impacts than seen in sites with infrequent fire.

5. Summary and Conclusions

This study has provided an assessment of albedo changes due to fire disturbance. With careful use of the consistently collected data provided by MODIS albedo products, a view of how fire disturbance can alter tundra land surface albedo was completed that provides insight into the potential impact of fire on energy exchange in this extensive biome. Fire decreases albedo in the sites studied substantially in the years following the burn. Severity differences between the two sites appear to influence the overall albedo change, at least in the first year following.

Limitations due to available albedo samples, restricted based on sun angle requirements for valid retrievals, require close attention to data quality and limit the analyses possible. However, further study could involve using the MODIS 1 day albedo (intermediate product) to look at the shoulder season albedo changes from fire to assess the impact of lower albedos on snowpack. Darker surfaces that could cause faster snow melt early and late in the snow season, or as suggested by *Rocha and Shaver* [2011a], might cause snow to persist longer due to changes in ground thermal regimes. These influences of surface modifications from fire could have additional lasting impacts on energy balance.

Tundra fire impacts on energy balance are different from the effects seen in boreal regions because summertime albedo change, not the influence of snow, is the main driver of the energy forcing in tundra. Also, the impact on growing season SSF in tundra is opposite to what is found in boreal regions and larger. While tundra fires are significantly smaller and less common than boreal fire, with increasing fire area and severity and the potentially large impact on growing season SSF, future fire in tundra could drive important energy balance modifications with regional and global consequences.

This study has shown that fire can cause a large change in SSF, especially at sites with severe burning. Extending results reported here and rigorously modeling fire's impact on SSF would allow a more in-depth assessment of the impact of future fire on local and regional energy balance. With projected increases in fire occurrence in tundra regions, albedo forcing from fire disturbance could be substantial enough to impact global-scale climate.

Acknowledgments

The satellite-derived spectral data used in this study (MCD43A3, Collection 005) are freely available from NASA-LPDAAC at https://lpdaac.usgs.gov/. Summary results of albedo are provided in the supporting information Table S2 and are the data used in the statistical assessment of albedo presented. The work presented was supported through grants from the NASA Terrestrial Ecology Program (grants NNX10AF41G and NNX13AK44G). The authors would like to acknowledge the help of Brian Thelen for assistance in the statistical modeling and analysis.

References

Arctic Climate Impact Assessment (2004), *Impacts of a Warming Arctic: Arctic Climate Impact Assessment*, Cambridge Univ. Press, Cambridge, U. K.

Alaska Interagency Coordination Center (2015), Historical Fire Information for Alaska. [Available at http://fire.ak.blm.gov/aicc.php, Accessed 1 August 2015.]

Barnes, C. A., and D. P. Roy (2010), Radiative forcing over the conterminous United States due to contemporary land cover use change and sensitivity to snow and interannual albedo variability, *J. Geophys. Res.*, *115*, G04033, doi:10.1029/2010JG001428.

Betts, A. K., and J. H. Ball (1997), Albedo over the boreal forest, *J. Geophys. Res.*, *102*, 28,901–28,909, doi:10.1029/96JD03876.

Betts, R. A. (2000), Offset of the potential carbon sink from boreal forestation by decreases in surface albedo, *Nature*, *408*(6809), 187–190.

Bret-Harte, M. S., M. C. Mack, G. R. Shaver, D. C. Huebner, M. Johnston, C. A. Mojica, C. Pizano, and J. A. Reiskind (2013), The response of Arctic vegetation and soils following an unusually severe tundra fire, *Philos. Trans. R. Soc. B*, *368*, 20120490, doi:10.1098/rstb.2012.0490.

Circumpolar Arctic Vegetation Map Team (2003), Circumpolar Arctic Vegetation Map, Scale 1:7,500,000, Conservation of Arctic Flora and Fauna (CAFF) Map No. 1, U. S. Fish and Wildl. Serv., Anchorage, Alaska. [Available at http://www.geobotany.uaf.edu/cavm/, Accessed 1 August 2014.]

Cescatti, A., et al. (2012), Intercomparison of MODIS albedo retrievals and in situ measurements across the global FLUXNET network, *Remote Sens. Environ.*, *121*, 323–334, doi:10.1016/j.rse.2012.02.019.

Chambers, S. D., J. Beringer, J. T. Randerson, and F. S. Chapin III (2005), Fire effects on net radiation and energy partitioning: Contrasting responses of tundra and boreal forest ecosystems, *J. Geophys. Res.*, *110*, D09106, doi:10.1029/2004JD005299.

Chapin, F. S., III, L. A. Viereck, P. C. Adams, K. Van Cleve, C. L. Fastie, R. A. Ott, D. Mann, and J. F. Johnstone (2006), Successional processes in the Alaskan Boreal Forest, in *Alaska's Changing Boreal Forest*, edited by F. S. Chapin III et al., chap. 7, pp. 100–120, Oxford Univ. Press, New York.

Eugster, W., et al. (2000), Land-atmosphere energy exchange in Arctic tundra and boreal forest: Available data and feedbacks to climate, *Global Change Biol.*, *6*(Suppl. 1), 84–115, doi:10.1046/j.1365-2486.2000.06015.x.

French, N. H. F. (2002), The impact of fire disturbance on carbon and energy exchange in the Alaskan boreal region: A geospatial analysis, PhD Dissertation thesis, 105 pp., Univ. of Michigan, Ann Arbor.

French, N. H. F., L. K. Jenkins, T. V. Loboda, M. Flannigan, R. Jandt, L. L. Bourgeau-Chavez, and M. Whitley (2015), Fire in arctic tundra of Alaska: Past fire activity, future fire potential, and significance for land management and ecology, *Int. J. Wildland Fire*, *24*(8), 1045–1061, doi:10.1071/WF14167.

Grosse, G., et al. (2011), Vulnerability of high latitude soil organic carbon in North America to disturbance, *J. Geophys. Res.*, *116*, G00K06, doi:10.1029/2010JG001507.

Hu, F. S., P. E. Higuera, J. E. Walsh, W. L. Chapman, P. A. Duffy, L. B. Brubaker, and M. L. Chipman (2010), Tundra burning in Alaska: Linkages to climatic change and sea ice retreat, *J. Geophys. Res.*, *115*, G04002, doi:10.1029/2009JG001270.

Huang, S., D. Dahal, H. Liu, S. Jin, C. Young, S. Li, and S. Liu (2015), Spatiotemporal variation of surface shortwave forcing from fire-induced albedo change in interior Alaska, *Can. J. For. Res.*, *45*, 276–285, doi:10.1139/cjfr-2014-0309.

Huntington, H. P., M. Boyle, G. E. Flowers, J. W. Weatherly, L. C. Hamilton, L. Hinzman, and J. Overpeck (2007), The influence of human activity in the Arctic on climate and climate impacts, *Clim. Change*, *82*(1–2), 77–92, doi:10.1007/s10584-006-9162-y.

Jandt, R., K. Joly, C. R. Meyers, and C. Racine (2008), Slow recovery of lichen on burned caribou winter range in Alaska tundra: Potential influences of climate warming and other disturbances, *Arct. Antarct. Alp. Res.*, *40*(1), 89–95, doi:10.1657/1523-0430(06-122)[JANDT]2.0.CO;2.

Jenkins, L. K., L. L. Bourgeau-Chavez, N. H. F. French, T. V. Loboda, and B. J. Thelen (2014), Development of methods for detection and monitoring of fire disturbance in the Alaskan tundra using a two-decade long record of synthetic aperture radar satellite images, *Remote Sens.*, *6*, 6347–6364, doi:10.3390/rs6076347.

Jin, Y., and D. P. Roy (2005), Fire-induced albedo change and its radiative forcing at the surface in northern Australia, *Geophys. Res. Lett.*, *32*, L13401, doi:10.1029/2005GL022822.

Jin, Y., C. B. Schaaf, C. E. Woodcock, F. Gao, X. Li, A. H. Strahler, W. Lucht, and S. Liang (2003), Consistency of MODIS surface bidirectional reflectance distribution function and albedo retrievals: 2. Validation, *J. Geophys. Res.*, *108*(D5), 4159, doi:10.1029/2002JD002804.

Jin, Y., J. T. Randerson, M. L. Goulden, and S. J. Goetz (2012), Post-fire changes in net shortwave radiation along a latitudinal gradient in boreal North America, *Geophys. Res. Lett.*, *39*, L13403, doi:10.1029/2012GL051790.

Jones, B. M., C. A. Kolden, R. Jandt, J. T. Abatzoglou, F. Urban, and C. D. Arp (2009), Fire behavior, weather, and burn severity of the 2007 Anaktuvuk River tundra fire, North Slope, Alaska, *Arct. Antarct. Alp. Res.*, *41*(3), 309–316, doi:10.1657/1938-4246-41.3.309.

Kasischke, E. S., D. Williams, and D. Barry (2002), Analysis of the patterns of large fires in the boreal forest region of Alaska, *Int. J. Wildland Fire*, *11*, 131–144, doi:10.1071/WF02023.

Liu, J., C. Schaaf, A. Strahler, Z. Jiao, Y. Shuai, Q. Zhang, M. Roman, J. A. Augustine, and E. G. Dutton (2009), Validation of Moderate Resolution Imaging Spectroradiometer (MODIS) albedo retrieval algorithm: Dependence of albedo on solar zenith angle, *J. Geophys. Res.*, *114*, D01106, doi:10.1029/2008JD009969.

Loboda, T., and I. Csiszar (2007), Reconstruction of fire spread within wildland fire events in Northern Eurasia from the MODIS active fire product, *Global Planet. Change*, *56*(3–4), 258–273, doi:10.1016/j.gloplacha.2006.07.015.

Loboda, T. V., N. H. F. French, C. Hight-Harf, L. K. Jenkins, and M. E. Miller (2013), Mapping fire extent and burn severity in Alaskan tussock tundra: An analysis of the spectral response of tundra vegetation to wildland fire, *Remote Sens. Environ.*, *134*, 194–209, doi:10.1016/j.rse.2013.03.003.

Loranty, M. M., S. J. Goetz, and P. S. A. Beck (2011), Tundra vegetation effects on pan-Arctic albedo, *Environ. Sci. Lett.*, *6*(2), 024014, doi:10.1088/1748-9326/6/2/029601.

Modern-Era Retrospective Analysis for Research and Applications (2013), Modern-era retrospective analysis for research and applications. [Available at http://gmao.gsfc.nasa.gov/research/merra/, Accessed 7-7-2015.]

Monson, R., and D. Baldocchi (2014), *Terrestrial Biosphere-Atmosphere Fluxes*, 486 pp., Cambridge Univ. Press, Cambridge, U. K.

Nowacki, G., P. Spencer, M. Fleming, T. Brock, and T. Jorgenson (2001), Ecoregions of Alaska*, map*, *U.S. Geol. Surv. Open-File Rep. 02-297*, U.S. Geol. Surv., Anchorage, Alaska.

Racine, C., J. L. Allen, and J. G. Dennis (2006), Long-term monitoring of vegetation change following tundra fires in Noatak National Preserve, Alaska, 37 pp., Arct. Network of Parks Inventory and Monit. Program, Natl. Park Serv., Alaska Region.

Racine, C. H., J. G. Dennis, and W. A. Patterson III (1985), Tundra fire regimes in the Noatak River watershed, Alaska: 1956–83, *Arctic*, *38*, 194–200.

Racine, C. H., L. A. Johnson, and L. A. Viereck (1987), Patterns of vegetation recovery after tundra fires in northwestern Alaska, U.S.A., *Arct. Alp. Res.*, *19*, 461–469.

Racine, C. H., R. R. Jandt, C. R. Meyers, and J. Dennis (2004), Tundra fire and vegetation change along a hillslope on the Seward Peninsula, Alaska, U.S.A., *Arct. Antarct. Alp. Res.*, *36*, 1–10, doi:10.1657/1523-0430(2004)036[0001:TFAVCA]2.0.CO;2.

Randerson, J. T., et al. (2006), The impact of boreal forest fire on climate warming, *Science*, *314*, 1130–1132, doi:10.1126/science.1132075.

Rocha, A. V., and G. R. Shaver (2011a), Postfire energy exchange in arctic tundra: The importance and climatic implications of burn severity, *Global Change Biol.*, *17*, 2831–2841, doi:10.1111/j.1365-2486.2011.02441.x.

Rocha, A. V., and G. R. Shaver (2011b), Burn severity influences postfire CO2 exchange in arctic tundra, *Ecol. Appl.*, *21*(2), 477–489, doi:10.1890/10-0255.

Rocha, A. V., M. M. Loranty, P. E. Higuera, M. C. Mack, F. S. Hu, B. M. Jones, A. L. Breen, E. B. Rastetter, S. J. Goetz, and G. R. Shaver (2012), The footprint of Alaskan tundra fires during the past half-century: Implications for surface properties and radiative forcing, *Environ. Sci. Lett.*, *7*, 044039, doi:10.1088/1748-9326/7/4/044039.

Roy, D. P., J. S. Borak, S. Devadiga, R. E. Wolfe, M. Zheng, and J. Descloitres (2002), The MODIS land product quality assessment approach, *Remote Sens. Environ.*, *83*, 62–76.

Schaaf, C. B., et al. (2002), First operational BRDF, albedo and nadir reflectance products from MODIS, *Remote Sens. Environ.*, *83*, 135–148.

Stow, D. A., et al. (2004), Remote sensing of vegetation and land-cover change in Arctic tundra ecosystems, *Remote Sens. Environ.*, *89*(3), 281–308.

Strahler, A. H., J. P. Muller, W. Lucht, C. B. Schaaf, T. Tsang, F. Gao, X. Li, P. Lewis, and M. J. Barnsley (1999), MODIS BRDF/albedo product: Algorithm theoretical basis document version 5.0. MODIS documentation. [Available at http://modis-land.gsfc.nasa.gov/pdf/atbd_mod09.pdf.]

Stroeve, J. C., J. E. Box, F. Gao, S. Liang, A. Nolin, and C. Schaaf (2005), Accuracy assessment of the MODIS 16-day albedo product for snow: Comparisons with Greenland in situ measurements, *Remote Sens. Environ.*, *94*(1), 46–60.

Sturm, M., T. Douglas, C. Racine, and G. E. Liston (2005), Changing snow and shrub conditions affect albedo with global implications, *J. Geophys. Res.*, *110*, G01004, doi:10.1029/2005JG000013.

Swann, A. L., I. Y. Fung, S. Levis, G. B. Bonan, and S. C. Doney (2010), Changes in Arctic vegetation amplify high-latitude warming through the greenhouse effect, *Proc. Natl. Acad. Sci. U.S.A.*, *107*(4), 1295–1300, doi:10.1073/pnas.0913846107.

Tape, K. E. N., M. Sturm, and C. Racine (2006), The evidence for shrub expansion in Northern Alaska and the Pan-Arctic, *Global Change Biol.*, *12*(4), 686–702, doi:10.1111/j.1365-2486.2006.01128.x.

Wang, Z., C. B. Schaaf, M. J. Chopping, A. H. Strahler, J. Wang, M. O. Roman, A. V. Rocha, C. E. Woodcock, and Y. Shuai (2012), Evaluation of Moderate-resolution Imaging Spectroradiometer (MODIS) snow albedo product (MCD43A) over tundra, *Remote Sens. Environ.*, *117*, 264–280.